Original Article

A novel method to perform morphological measurements on three-dimensional (3D) models of the calcaneus based on computed tomography (CT)-imaging

Alexander M. Wakker[1,2], Esther M. M. Van Lieshout[1], A. Siebe De Boer[1], Bart M. W. Cornelissen[3], Michael H. J. Verhofstad[1], Theo Van Walsum[4], Jacob J. Visser[2], Mark G. Van Vledder[1]

[1]Trauma Research Unit, Department of Surgery, Erasmus MC, University Medical Center Rotterdam, Rotterdam, The Netherlands; [2]Department of Radiology & Nuclear Medicine, Erasmus MC, University Medical Center Rotterdam, Rotterdam, The Netherlands; [3]Department of Oral and Maxillofacial Surgery, Erasmus MC, University Medical Center Rotterdam, Rotterdam, The Netherlands; [4]Biomedical Imaging Group Rotterdam, Department of Radiology & Nuclear Medicine, Erasmus MC, University Medical Center Rotterdam, Rotterdam, The Netherlands

Contributions: (I) Conception and design: AM Wakker, BMW Cornelissen, JJ Visser, MG Van Vledder; (II) Administrative support: EMM Van Lieshout, JJ Visser, MG Van Vledder; (III) Provision of study materials or patients: EMM Van Lieshout, AS De Boer, MHJ Verhofstad, T Van Walsum, JJ Visser, MG Van Vledder; (IV) Collection and assembly of data: AM Wakker, AS De Boer, MG Van Vledder; (V) Data analysis and interpretation: A Wakker, EMM Van Lieshout, BMW Cornelissen, T Van Walsum, JJ Visser, MG Van Vledder; (VI) Manuscript writing: All authors; (VII) Final approval of manuscript: All authors.

Correspondence to: Mark G. Van Vledder, MD, PhD. Trauma Research Unit, Department of Surgery, Erasmus MC, University Medical Center Rotterdam, Dr. Molewaterplein 40, 3015 GD Rotterdam, The Netherlands. Email: m.vanvledder@erasmusmc.nl; Alexander M. Wakker, MSc. Trauma Research Unit, Department of Surgery, Erasmus MC, University Medical Center Rotterdam, Dr. Molewaterplein 40, 3015 GD Rotterdam, The Netherlands; Department of Radiology & Nuclear Medicine, Erasmus MC, University Medical Center Rotterdam, Dr. Molewaterplein 40, 3015 GD Rotterdam, The Netherlands. Email: a.wakker@erasmusmc.nl.

Background: While current preoperative and postoperative assessment of the fractured and surgically reconstructed calcaneus relies on computed tomography (CT)-imaging, there are no established methods to quantify calcaneus morphology on CT-images. This study aims to develop a semi-automated method for morphological measurements of the calcaneus on three-dimensional (3D) models derived from CT-imaging.

Methods: Using CT data, 3D models were created from healthy, fractured, and surgically reconstructed calcanei. Böhler's angle (BA) and Critical angle of Gissane (CAG) were measured on conventional lateral radiographs and corresponding 3D CT reconstructions using a novel point-based method with semi-automatic landmark placement by three observers. Intraobserver and interobserver reliability scores were calculated using intra-class correlation coefficient (ICC). In addition, consensus among observers was calculated for a maximal allowable discrepancy of 5 and 10 degrees for both methods.

Results: Imaging data from 119 feet were obtained (40 healthy, 39 fractured, 40 reconstructed). Semi-automated measurements on 3D models of BA and CAG showed excellent reliability (ICC: 0.87–1.00). The manual measurements on conventional radiographs had a poor-to-excellent reliability (ICC: 0.22–0.96). In addition, the percentage of consensus among observers was much higher for the 3D method when compared to conventional two-dimensional (2D) measurements.

Conclusions: The proposed method enables reliable and reproducible quantification of calcaneus morphology in 3D models of healthy, fractured and reconstructed calcanei.

Keywords: Calcaneus; three-dimensional morphological measurements (3D morphological measurements); computed tomography (CT); observer reliability

Submitted Jan 25, 2024. Accepted for publication Mar 22, 2024. Published online Apr 17 2024.
doi: 10.21037/qims-24-142
View this article at: https://dx.doi.org/10.21037/qims-24-142

Introduction

Calcaneal fractures are predominantly caused by high-energy traumas, often resulting in complex fractures that require complex reconstructive surgery. Surgical treatment of calcaneus fractures and its sequelae such as calcaneus malunion, cannot be performed without proper preoperative, intraoperative, and postoperative imaging techniques. Traditional measures used to describe deformities of the fractured calcaneus and assess the quality of surgical reconstruction including Böhler's angle (BA) and the Critical angle of Gissane (CAG).

BA is determined by first drawing a line from the highest point of the posterior facet to the highest point of the calcaneal tuberosity, and then another line from the anterior process to the posterior facet, as illustrated in *Figure 1*. Typically, this angle ranges from 20° to 40° in non-fractured calcanei (1). Variations from this range can signal the degree of depression, the displacement of the subtalar joint, and the extent of deformity between the anterior and posterior portions of the calcaneus. The CAG is determined by the intersection of two lines within the calcaneal sulcus: one initiating from the anterior process and the other extending along the posterior facet (*Figure 1*). The literature presents a range of normal values for the CAG, with Anthony *et al.* (2) suggesting a range between 130° to 145°, while Keener *et al.* (3) offer a slightly broader span of 120° to 145°. Deviations from this range can reveal the extent of depression, the displacement of the subtalar joint, and the altered position of the posterior facet relative to the anterior process (3).

These measurements, derived from two-dimensional (2D) X-ray imaging (1,4), are easy to obtain and compute. Yet, despite their ease, their reliability and accuracy are often disputed due to significant inter- and intra-user variability (5-10), especially considering the narrow ranges these measurements typically fall into.

Computed tomography (CT) imaging has largely replaced or at least complemented X-ray as a tool to decide between non-operative and operative management, and in the latter on the optimal surgical technique, due to its superior three-dimensional (3D) information on calcaneus morphology and joint congruency. While 2D CT slices and 3D CT reconstructions allow surgeons and experienced radiologists to qualitatively assess the anatomy and morphology of fractures and surgically reconstructed calcanei, there are currently no established methods for the objective quantification and classification of CT imaging data of fractured and surgically reconstructed calcanei (11-16). Qiang *et al.* (11) demonstrated that manual 3D morphological measurements on 3D CT-imaging data from healthy calcanei is reliable and repeatable. However, the measurements were performed manually, which is time-consuming and might be prone to human error when performing the measurements on fractured and surgically reconstructed calcanei models. Idram *et al.* (15) introduced a method using Gaussian surface curvature for 3D measurements, but its accuracy depended heavily on the quality of the 3D model reconstruction. The method may be significantly influenced by inaccurate reconstructions, sharp edges of fractures or the presence of metal hardware in surgically reconstructed calcanei, which could greatly influence the Gaussian curvature calculation.

Further complicating the matter is the inherent unreliability of measurements performed directly on CT slices due to slice-dependent variability. A measurement performed on one slice may yield a result markedly different from measurements obtained from another slice, leading to inconsistencies and potential misinterpretations.

As the use of 3D CT imaging becomes increasingly prevalent in modern medical practice, there is a pressing need to develop reliable, efficient, and standardized measurement techniques based on this modality. This advancement could increase the accuracy and intraobserver and interobserver reliability of descriptions for calcaneus fractures and reconstructions, thus providing a more reliable basis for surgical planning. The purpose of this study is to equip surgeons and radiologists with a tool capable of semi-automatically and accurately performing 3D morphological measurements.

Therefore, the aim of this study was to develop and evaluate a novel method for performing 3D, semi-automated measurements of BA and the CAG on 3D models obtained from CT imaging data of healthy, fractured, and surgically reconstructed calcanei. We present this article in accordance with the GRRAS reporting

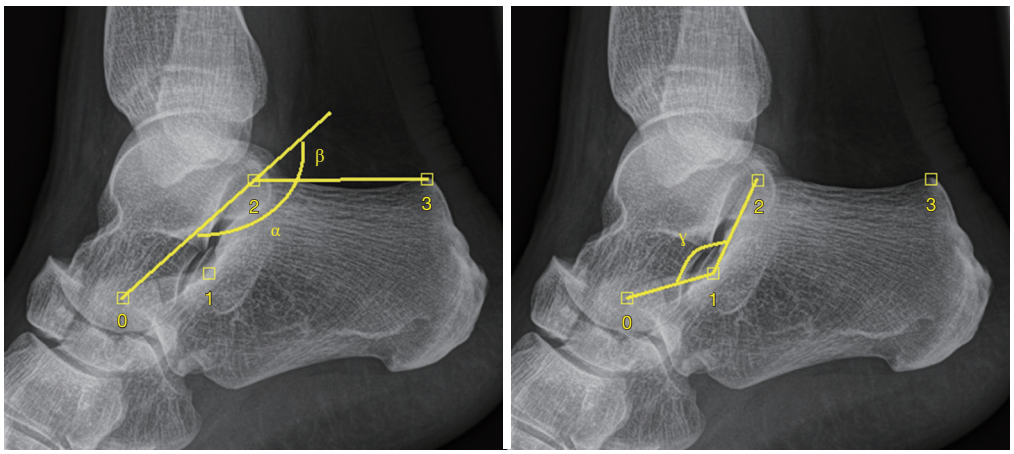

Figure 1 Selected landmarks to calculate Böhler's angle (β, left) and Critical angle of Gissane (ɣ, right) on conventional lateral radiographs. [0] The most superior point of the anterior process; [1] the most inferior point of the posterior facet; [2] the most superior point of the posterior facet; and [3] the most superior point of the calcaneal tuberosity.

checklist (available at https://qims.amegroups.com/article/view/10.21037/qims-24-142/rc).

Methods

This study was conducted in accordance with the Declaration of Helsinki (as revised in 2013). The study protocol was exempted by the local Medical Research Ethics Committee (No. MEC-2021-0529). Given the nature and design of the study, the committee granted a waiver for the requirement of informed consent from participants.

Semi-automated measurement of BA and the CAG

A semi-automated algorithm was developed in Python (3.9) to perform 3D measurements on 3D CT-based calcaneus models. Anatomical landmarks to perform the measurements were identified using constructed vectors based on the anatomical planes. The four landmarks to perform the measurements were: [0] the most superior point of the anterior process; [1] the most inferior point of the posterior facet; [2] the most superior point of the posterior facet; and [3] the most superior point of the calcaneal tuberosity (*Figure 1*). The algorithm selected the maximum value in the chosen bone surface region based on the vectors. Additionally, a Graphical User Interface (GUI) was developed in MevisLab™ to facilitate traditional manual 2D measurements and the semi-automated 3D measurements (*Figure 2*).

Patients

To test the algorithm, data from a single medical center were used. This study utilized existing conventional radiographs and CT scans of healthy, fractured (joint depression type) and reconstructed calcanei acquired at the Erasmus MC between January 1, 2006 and December 31, 2021. The inclusion criteria were: (I) both conventional radiographs and CT scans of the same foot were available, (II) interval between scans <6 months, (III) age ≥16 years. Patients with extra-articular (including tongue type fractures) or non-displaced fractures or patient that underwent subtalar arthrodesis were excluded. Measurements of BA and the CAG on 2D images and 3D models of the calcaneus were performed by two experienced orthopedic trauma surgeons and a senior resident in orthopedic trauma. All were well experienced in foot and ankle surgery and had experience in performing 2D morphological measurements on the calcaneus. Before use, all data was anonymized.

Preparation of 3D models

3D models were created from the CT scans using standard CT-segmentation methods such as a fixed bone threshold, smart fill, filling holes and cavities and wrapping as available in the Materialise Mimics software package, version 24.0 (Materialise, Leuven, Belgium).

Thereafter, the spatial orientation of the 3D models was determined. First, an experienced, musculoskeletal radiologist determined the sagittal, axial and coronal planes

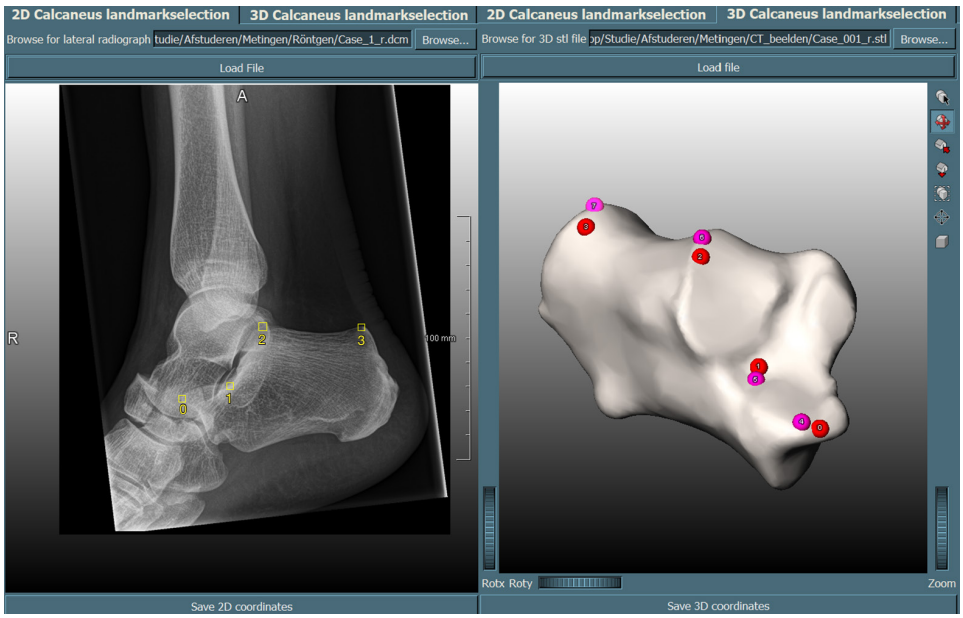

Figure 2 Screenshot of the developed Graphical User Interface to measure Böhler angle and the Critical angle of Gissane. (Left) two-dimensional radiographs measurements on the calcaneus; (right) 3D measurements on 3D models of the calcaneus. The selected landmarks by the observers are depicted with red, and the corrected landmarks by the algorithm with purple. [0] The most superior point of the anterior process; [1] the most inferior point of the posterior facet; [2] the most superior point of the posterior facet; and [3] the most superior point of the calcaneal tuberosity; [4] the most superior point of the anterior process corrected by the algorithm; [5] the most inferior point of the posterior facet by the algorithm; [6] the most superior point of the posterior facet by the algorithm; [7] the most superior point of the calcaneal tuberosity by the algorithm. 2D, two-dimensional; 3D, three-dimensional.

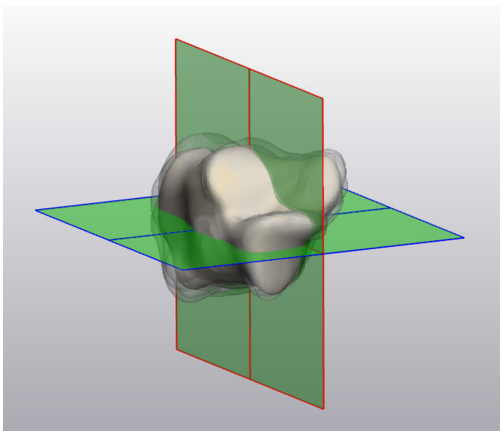

Figure 3 Example of orientation of healthy calcanei models (transparent) with the anatomical planes of the three-dimensional mean shape model (opaque) of the calcaneus.

of a mean shape model of the left and right calcaneus. The mean shape models were constructed from 88 individual 3D calcanei models. Each calcaneus model was rigidly aligned using point-to-point Iterative Closest Point (ICP) registration to a standard reference frame of the calcaneus. Thereafter, the reference frame was non-rigidly wrapped around each of the calcanei models to standardize the topology across the 3D calcanei models. Principle Component Analysis was then applied to the aligned models to extract the mean shape model of the calcaneus. Next, the 3D models were aligned with the fixed mean shape models of the calcaneus. This was performed using a rigid point-to-point ICP registration, which minimizes the root mean square distance between the points of the models (*Figure 3*).

Measurements on 2D X-ray images and 3D models

After a brief training on how to perform the measurements in the GUI, all three participants determined BA and the CAG on the lateral radiographs (*Figure 1*) and the 3D models (*Figure 4*) based on the previously mentioned landmarks. For the 3D measurements, participants first selected initial markers in the region of the landmarks, after which these markers were automatically replaced

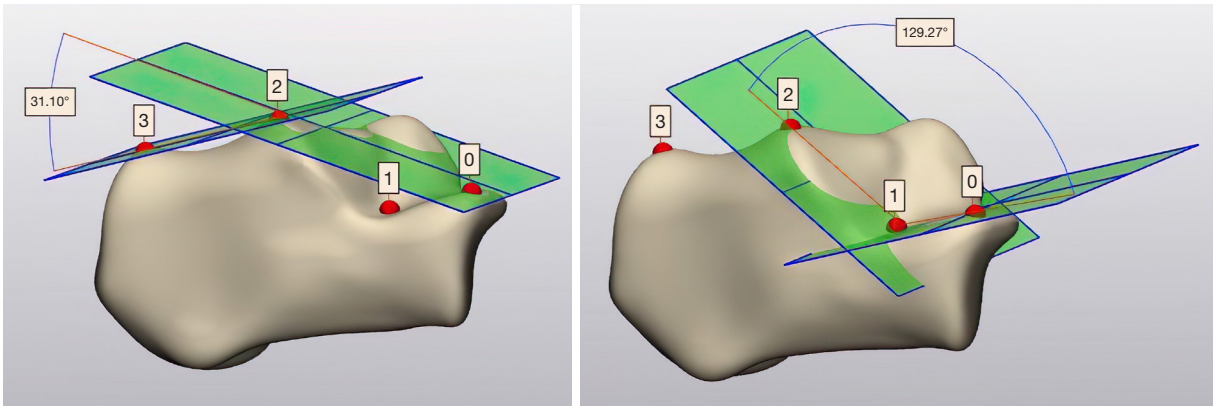

Figure 4 Böhler's angle in 3D (left) and the Critical angle of Gissane in 3D (right). [0] The most superior point of the anterior process; [1] the most inferior point of the posterior facet; [2] the most superior point of the posterior facet; and [3] the most superior point of the calcaneal tuberosity. 3D, three-dimensional.

by the most superior or inferior points on the given structures (*Figure 2*). Lastly, the corrected landmarks were orthogonally projected onto the sagittal plane to enable the creation of planes between the selected landmarks for calculation of BA and the CAG (*Figure 4*). All measurements were repeated independently by the same participants one week after the initial measurements to assess the intraobserver variability. The time required to perform both 2D and 3D measurements was comparable, as the algorithm efficiently adjusted the selected landmarks in under a second, making the difference in duration between the two methods negligible.

Sample size calculation

The sample size needed to determine the intraobserver and interobserver reliability was calculated using an online intra-class correlation coefficient (ICC) hypothesis testing calculator (17), which used a method developed by Walter *et al.* (18). The minimum sample size for each population was 37. The sample size was calculated assuming the following variables: 3 observers, significance level (alpha) of 0.05, power of 0.90 (beta 0.10), minimum acceptable reliability of 0.65, expected reliability of 0.85, and potential drop-out of 10%.

Comparison of the 2D and 3D measurement methods

To determine if the methods to perform the 2D and 3D measurements agree sufficiently closely, the Bland-Altman approach was used (19). The mean difference between the 2D and 3D measurements and standard deviation of the difference were calculated. Additionally, the mean and median 2D and 3D measurements of BA and the CAG were calculated.

ICC

Data were analyzed using IBM SPSS Statistics for Windows, version 25 (IBM Corp., Armonk, NY, USA). The reliability of the morphological measurements was determined by using the interobserver and intraobserver reliability. To measure the reliability, the ICCs was calculated. The ICC score for the interobserver and intraobserver reliability was calculated assuming a two-way mixed model and an one-way random model with measures of consistency and a confidence interval of 95%, respectively (20,21). The ICC is a value between 0 and 1, and can be interpreted as follows: 0.00–0.50 poor reliability, 0.50–0.75 moderate reliability, 0.75–0.90 good reliability, 0.90–1.00 excellent reliability (22). Because the ICC does not show the exact differences in measurements made by observers, the percentage of measurements within acceptable error margins was calculated for BA and the CAG. Acceptable discrepancies were set at 5, 10, 20, 30, 50, and 70 degrees.

Results

Measurements were performed on a total of 119 lateral foot radiographs and corresponding CT scans, consisting

Table 1 Morphological parameters of 2D and 3D measurements of Böhler's angle

Patient type	2D Böhler's angle				3D Böhler's angle			
	Mean (SD)	Median (P_{25}–P_{75})	Min	Max	Mean (SD)	Median (P_{25}–P_{75})	Min	Max
Healthy	31.47 (5.84)	32.15 (27.40–35.81)	16.64	44.10	29.94 (5.06)	30.58 (26.17–33.27)	18.10	42.72
Fractured	3.98 (18.35)	6.57 (–1.82–14.22)	–48.98	42.80	14.39 (14.70)	15.73 (10.92–22.58)	–45.17	38.58
Reconstructed	24.19 (10.55)	25.61 (18.21–30.02)	–8.58	62.08	25.54 (9.99)	25.29 (19.97–31.71)	2.36	51.92

2D, two-dimensional; 3D, three-dimensional; SD, standard deviation.

Table 2 Morphological parameters of 2D and 3D measurements of the Critical angle of Gissane

Patient type	2D Gissane's angle				3D Gissane's angle			
	Mean (SD)	Median (P_{25}–P_{75})	Min	Max	Mean (SD)	Median (P_{25}–P_{75})	Min	Max
Healthy	123.33 (7.64)	122.56 (118.45–129.39)	102.49	147.25	128.15 (6.15)	127.25 (124.45–132.76)	112.87	147.36
Fractured	125.11 (14.13)	125.79 (116.08–134.29)	78.62	165.07	117.59 (15.59)	119.77 (108.64–128.53)	72.53	144.05
Reconstructed	127.64 (9.99)	127.18 (122.22–133.11)	96.62	163.83	127.10 (12.17)	128.41 (118.50–136.13)	96.33	151.81

2D, two-dimensional; 3D, three-dimensional; SD, standard deviation.

Table 3 ICC for 2D Böhler's angle measurements

ICC 2D Böhler's angle	Healthy calcaneus		Fractured calcaneus		Reconstructed calcaneus	
	ICC (95% CI)	Agreement	ICC (95% CI)	Agreement	ICC (95% CI)	Agreement
Interobserver reliability						
First measurement	0.79 (0.68–0.88)	M–G	0.83 (0.73–0.90)	M–G	0.83 (0.73–0.90)	M–G
Second measurement	0.75 (0.63–0.85)	M–G	0.84 (0.75–0.91)	G–E	0.86 (0.78–0.92)	G–E
Intraobserver reliability						
Observer 1	0.92 (0.85–0.96)	G–E	0.93 (0.88–0.96)	G–E	0.90 (0.82–0.95)	G–E
Observer 2	0.76 (0.59–0.86)	M–G	0.70 (0.50–0.83)	M–G	0.88 (0.79–0.93)	G–E
Observer 3	0.83 (0.69–0.90)	M–G	0.96 (0.77–0.93)	G–E	0.89 (0.81–0.94)	G–E

ICC, intra-class correlation coefficient; 2D, two-dimensional; G, good; M, moderate; E, excellent; CI, confidence interval.

of 40 healthy, 39 fractured, and 40 reconstructed calcanei. *Tables 1* and *2* display the mean and median 2D and 3D measurements of BA and the CAG, respectively.

Comparison 2D and 3D measurement methods

In the non-fractured group, the mean differences between the 2D and 3D measurements were 1.5 (SD: 3.5) and –4.8 (SD: 7.1) degrees for the BA and CAG, respectively. For the fractured group, the mean differences were –10.4 (SD: 13.3) and 7.5 (SD: 14.7) degrees for the BA and CAG, respectively. In the surgically reconstructed group, the differences between the two methods were –1.4 (SD: 9.9) and 0.5 (SD: 12.2) degrees for the BA and CAG, respectively.

Reliability measurements of BA and CAG

ICC scores for 2D and 3D measurements varied across different states of calcanei. For 2D measurements, BA interobserver reliability ranged from 0.77–0.85, while intraobserver reliability ranged from 0.84–0.89 (*Table 3*). For 3D measurements, both interobserver and intraobserver reliability showed excellent scores (0.93–1.00) (*Table 4*).

The CAG measurements in 2D showed an interobserver reliability ranging from 0.44–0.61 and intraobserver

Table 4 ICC for 3D Böhler's angle measurements

ICC 3D Böhler's angle	Healthy calcaneus		Fractured calcaneus		Reconstructed calcaneus	
	ICC (95% CI)	Agreement	ICC (95% CI)	Agreement	ICC (95% CI)	Agreement
Interobserver reliability						
First measurement	1.00 (0.99–1.00)	E	0.99 (0.98–0.99)	E	0.99 (0.99–1.00)	E
Second measurement	1.00 (1.00–1.00)	E	0.99 (0.98–0.99)	E	0.98 (0.97–0.99)	E
Intraobserver reliability						
Observer 1	1.00 (1.00–1.00)	E	0.99 (0.98–0.99)	E	0.97 (0.95–0.99)	E
Observer 2	1.00 (1.00–1.00)	E	0.99 (0.93–0.99)	E	0.99 (0.99–1.00)	E
Observer 3	0.99 (0.99–1.00)	E	0.98 (0.97–0.99)	E	0.99 (0.99–1.00)	E

ICC, intra-class correlation coefficient; 3D, three-dimensional; E, excellent; CI, confidence interval.

Table 5 ICC for 2D Critical angle of Gissane measurements

ICC 2D Critical angle of Gissane	Healthy calcaneus		Fractured calcaneus		Reconstructed calcaneus	
	ICC (95% CI)	Agreement	ICC (95% CI)	Agreement	ICC (95% CI)	Agreement
Interobserver reliability						
First measurement	0.59 (0.41–0.74)	P–M	0.41 (0.22–0.60)	P–M	0.52 (0.33–0.68)	P–M
Second measurement	0.62 (0.45–0.76)	P–G	0.46 (0.26–0.64)	P–M	0.52 (0.33–0.68)	P–M
Intraobserver reliability						
Observer 1	0.75 (0.58–0.86)	M–G	0.88 (0.79–0.94)	G–E	0.62 (0.39–0.78)	P–G
Observer 2	0.81 (0.66–0.89)	M–G	0.22 (0.00–0.50)	P–M	0.54 (0.28–0.73)	P–M
Observer 3	0.79 (0.64–0.89)	M–G	0.47 (0.19–0.68)	P–M	0.38 (0.08–0.62)	P–M

ICC, intra-class correlation coefficient; 2D, two-dimensional; P, poor; M, moderate; G, good; E, excellent; CI, confidence interval.

reliability from 0.51–0.78 (*Table 5*). In contrast, measurements in 3D demonstrated good-to-excellent interobserver and intraobserver reliability (0.76–0.98) (*Table 6*).

At a 5-degree discrepancy, 2D BA measurements achieved consensus rates of 75% for healthy, 36% for fractured, and 44% for reconstructed calcanei. For 2D CAG measurements this was 31%, 14% and 21%, respectively. These rates improved with a 10-degree discrepancy to 94%, 71%, and 77% for BA, and 70%, 41%, and 53% for CAG (*Figure 5A*,*5B*). Meanwhile, 3D measurements maintained high consensus rates at both 5-degree (BA: 100% healthy, 87% fractured, 97% reconstructed; CAG: 89%, 81%, and 73%) (*Figure 6A*) and 10-degree discrepancies (BA: 100% for healthy and fractured, 99% reconstructed; CAG: 100%, 81%, and 95%) (*Figure 6B*).

Discussion

In this study, conventional 2D radiograph BA and CAG measurements on healthy, fractured, and surgically reconstructed calcanei were compared to 3D measurements acquired using a newly developed semi-automated method based on CT imaging data.

The results showed that there is moderate-to-excellent and poor-to-good interobserver and intraobserver reliability for the 2D BA and CAG measurements, respectively. Especially for the fractured calcanei, reliability was generally poor. The semi-automatic method to perform the 3D morphological measurements performed excellent for both healthy, fractured, and surgically reconstructed calcanei.

It is important to note that the 2D and 3D measurements were taken from the same individuals, allowing for a direct

Table 6 ICC for 3D Critical angle of Gissane measurements

ICC 3D Critical angle of Gissane	Healthy calcaneus		Fractured calcaneus		Reconstructed calcaneus	
	ICC (95% CI)	Agreement	ICC (95% CI)	Agreement	ICC (95% CI)	Agreement
Interobserver reliability						
First measurement	0.94 (0.91–0.97)	E	0.96 (0.93–0.98)	E	0.95 (0.91–0.97)	E
Second measurement	0.92 (0.87–0.96)	G–E	0.89 (0.82–0.94)	G–E	0.95 (0.91–0.97)	E
Intraobserver reliability						
Observer 1	0.94 (0.88–0.97)	G–E	0.87 (0.77–0.93)	G–E	0.92 (0.85–0.96)	G–E
Observer 2	0.95 (0.91–0.97)	E	0.87 (0.76–0.93)	G–E	0.94 (0.89–0.97)	G–E
Observer 3	0.91 (0.83–0.95)	G–E	0.95 (0.91–0.97)	E	0.96 (0.93–0.98)	E

ICC, intra-class correlation coefficient; 3D, three-dimensional; E, excellent; G, good; CI, confidence interval.

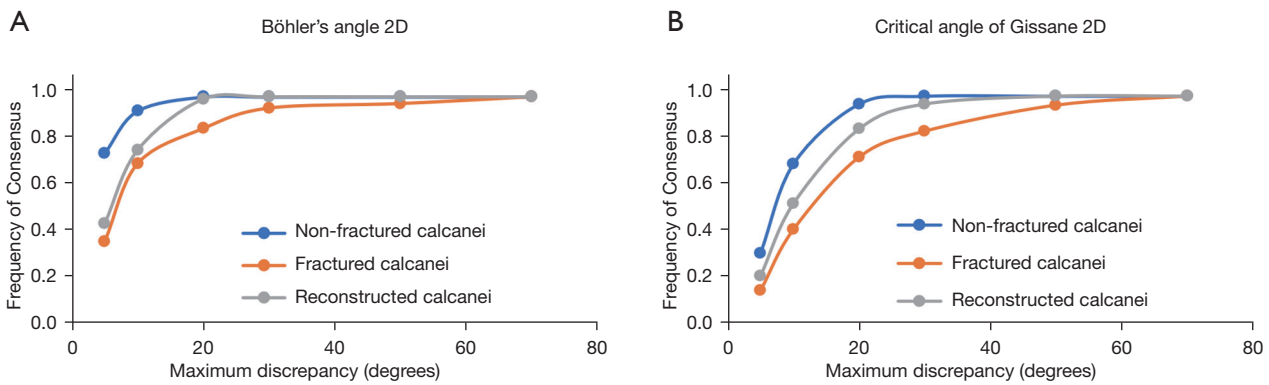

Figure 5 The frequency of Consensus given an allowable discrepancy for the two-dimensional measurements of Böhler's angle (A) and the Critical angle of Gissane (B) between the observers. 2D, two-dimensional.

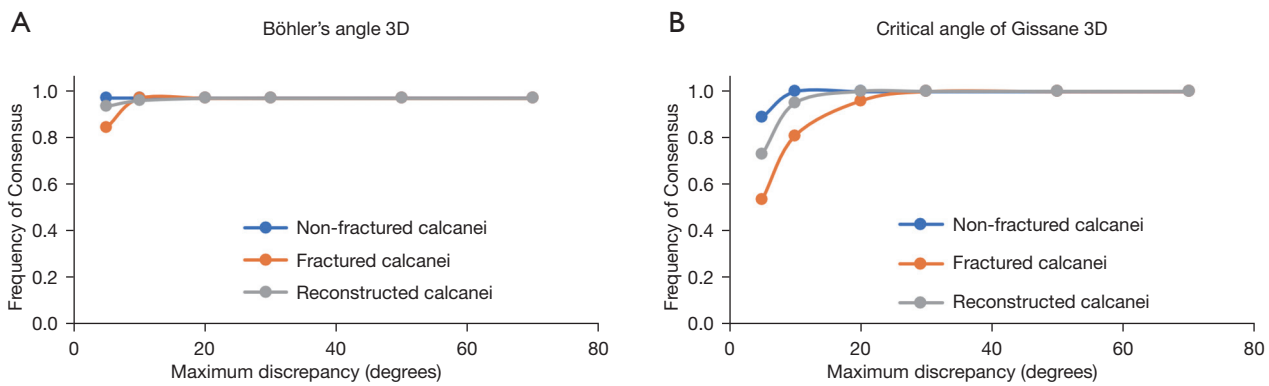

Figure 6 The frequency of Consensus given an allowable discrepancy for the three-dimensional measurements of Böhler's angle (A) and the Critical angle of Gissane (B) between the observers. 3D, three-dimensional.

comparison at an individual level. There were minor differences between the 2D and 3D measurements in the non-fractured group, suggesting a generally good agreement between these methods. In contrast, the fractured group showed a large mean difference and large standard deviation, suggesting potential bias and high variability. Although the surgically reconstructed group had small mean difference, the standard deviation was large. This disparity in standard deviation suggests significant variability between individual outcomes. Such individual variations imply that directly comparing 2D and 3D measurements may not be sufficient for the fractured and surgically reconstructed population. A separate evaluation of the 2D and 3D measurements suggested that 3D measurements, derived from 3D models, yield more accurate and consistent results, likely due to the superior intraobserver and interobserver reliability associated with the 3D measurements.

Prior studies have reported the reliability and reproducibility of morphologic measurements in 2D radiographs of the calcaneus (5-10). Where reasonably good results regarding the interobserver and intraobserver reliability can be obtained in non-fractured calcanei, this is much less the case for fractured and reconstructed calcanei. For instance, Otero *et al.* (10) reported that lateral radiographs have inherent limitations in their interpretation when measured on fractured calcanei. They found comparable results to our study for measuring BA, but a lower score for the CAG, with a mean interobserver ICC of 0.80 *vs.* 0.83 for BA and 0.19 *vs.* 0.43 for the CAG in fractured calcanei.

The presented method, although not fully automated, enhances the intraobserver and interobserver reliability of BA and CAG measurements by minimizing human error in landmark placements. Techniques like the one presented could be part of an automatic radiological reporting system. (Semi-)automatic radiological reporting can accelerate the image analysis process and minimize the need for manual intervention, thus reducing both error and time while increasing consistency and therefore quality. This would enhance the precision of the measurements and their reproducibility, providing a more consistent basis for diagnosis, treatment planning, and patient outcomes.

It is also essential to introduce new terminology that accurately reflects CT-based findings, since the existing measurements like BA and CAG were conceived from 2D imaging. Furthermore, beyond the constraints of 2D, we suggest investigating quantifiable 3D parameters for a more accurate representation of the calcaneus morphology, such as posterior talocalcaneal joint- and calcaneocuboid joint-incongruity, and varus/valgus angulation. These parameters can offer a more comprehensive understanding of the calcaneus' complex 3D shape, and could potentially provide a better basis for understanding its biomechanical behavior, pathology, and response to treatment.

Limitations of this study include the relatively small sample size. Furthermore, while the semi-automated algorithm can improve the reliability and reproducibility of the measurements, it still relies on the initial placement of landmarks by the observer, which might still introduce some variability. In addition, the segmentation and orientation were not fully automated, which might influence the reproducibility due to human variation. Lastly, clinical significance of the improved intraobserver and interobserver reliability of the 3D measurements has not been established and would require further investigation in prospective evaluations.

We hypothesize that the methodology presented in this paper can be easily adapted to quantify the morphology of other bony structures such as the femur, tibia, radius, ulna, etc. For example, this algorithm could be utilized to measure femoral neck-shaft angle, radial volar/dorsal angulation, radial shift, and ulnar variance. By integrating these additional measurements, the algorithm's applications can be expanded to assess and analyze a wider range of skeletal structures and their associated clinical implications.

Conclusions

In conclusion, the current study presents a semi-automated method which reliably performs morphological measurements on CT-based 3D models of the calcaneus.

Acknowledgments

This work partially contained A.M.W.' Master thesis from the TU Delft Mechanical, Maritime and Materials Engineering. The thesis can be downloaded at: https://repository.tudelft.nl/islandora/object/uuid%3A3f1327b1-1836-4b47-9765-c654d27ec246. The authors also wish to clarify that, according to the regulations of TU Delft, copyright on bachelor's and master's theses or any other student work created during the period of study is retained by the student, unless specific written agreements stating otherwise exist. A.M.W. has granted permission for the use of his Master thesis as part of this work, and all necessary documentation regarding this permission has been provided

to the Editorial Office to avoid potential copyright risks.
Funding: This study was financially supported by the Osteosynthesis & Trauma Care Foundation (OTC) (No. 2022-JDMV, to A.M.W.).

Footnote

Reporting Checklist: The authors have completed the GRRAS reporting checklist. Available at https://qims.amegroups.com/article/view/10.21037/qims-24-142/rc

Conflicts of Interest: All authors have completed the ICMJE uniform disclosure form (available at https://qims.amegroups.com/article/view/10.21037/qims-24-142/coif). A.M.W. reports that he received funding from Ostheosynthesis & Trauma Care Foundation for research about the calcaneus. The other authors have no conflicts of interest to declare.

Ethical Statement: The authors are accountable for all aspects of the work in ensuring that questions related to the accuracy or integrity of any part of the work are appropriately investigated and resolved. The study was conducted in accordance with the Declaration of Helsinki (as revised in 2013). The study protocol was exempted by the local Medical Research Ethics Committee (No. MEC-2021-0529). Given the nature and design of the study, the committee granted a waiver for the requirement of informed consent from participants.

References

1. Davis D, Seaman TJ, Newton EJ. Calcaneus Fractures. In: StatPearls [Internet]. Treasure Island (FL): StatPearls Publishing; Date of access: 03-01-2022. Available online: https://www.ncbi.nlm.nih.gov/books/NBK430861/
2. Anthony J. Critical angle of gissane: How to use in the diagnosis of a calcaneus fracture. ebm consult. Data of access 10-15-2021. Available online: https://www.ebmconsult.com/articles/critical-angle-gissane-calcaneus-fractures
3. Keener BJ, Sizensky JA. The anatomy of the calcaneus and surrounding structures. Foot Ankle Clin 2005;10:413-24.
4. Daftary A, Haims AH, Baumgaertner MR. Fractures of the calcaneus: a review with emphasis on CT. Radiographics 2005;25:1215-26.
5. Knight JR, Gross EA, Bradley GH, Bay C, LoVecchio F. Boehler's angle and the critical angle of Gissane are of limited use in diagnosing calcaneus fractures in the ED. Am J Emerg Med 2006;24:423-7.
6. Sayed-Noor AS, Agren PH, Wretenberg P. Interobserver reliability and intraobserver reproducibility of three radiological classification systems for intra-articular calcaneal fractures. Foot Ankle Int 2011;32:861-6.
7. Dos Santos Barroso R, de Miranda BR, Fernandes HA, Pessoa GB, Nishikawa DRC, de Oliveira LZP, de Freitas ADP, de Almeida CI. Inter-rater reliability of Böhler and Gissane angles in different calcaneal fracture according to the Essex-Lopresti and Sanders classifications. J Foot Ankle 2021;15:133-9.
8. Labronici PJ, Faria GGP, Pedro BM, Serra MDFA, Pires RES, Tamontini JL. Böhler's Angle-Comparison Between the pre- and Postoperative in Displaced Intra-Articular Calcaneal Fractures. Rev Bras Ortop (Sao Paulo) 2019;54:156-64.
9. Bulut T, Gursoy M. Are radiological measurements reliable methods in the postoperative follow-up of calcaneal fractures? Niger J Clin Pract 2021;24:110-4.
10. Otero JE, Westerlind BO, Tantavisut S, Karam MD, Phisitkul P, Akoh CC, Gao Y, Marsh JL. There is poor reliability of Böhler's angle and the crucial angle of Gissane in assessing displaced intra-articular calcaneal fractures. Foot Ankle Surg 2015;21:277-81.
11. Qiang M, Chen Y, Zhang K, Li H, Dai H. Measurement of three-dimensional morphological characteristics of the calcaneus using CT image post-processing. J Foot Ankle Res 2014;7:19.
12. Melinska AU, Romaszkiewicz P, Wagel J, Sasiadek M, Iskander DR. Statistical, Morphometric, Anatomical Shape Model (Atlas) of Calcaneus. PLoS One 2015;10:e0134603.
13. Qiang M, Chen Y, Jia X, Zhang K, Li H, Jiang Y, Zhang Y. Post-operative radiological predictors of satisfying outcomes occurring after intra-articular calcaneal fractures: a three dimensional CT quantitative evaluation. Int Orthop 2017;41:1945-51.
14. Irwansyah, Lai JY, Essomba T, Lee PY. Measurement

and Analysis of Calcaneus Morphometric Parameters from Computed Tomography Images. ICBBE '18: Proceedings of the 2018 5th International Conference on Biomedical and Bioinformatics Engineering. Association for Computing Machinery Irwansyah: Okinawa, Japan, 2018:82-6.
15. Idram I, Lai JY, Lee PY. A reliable method for morphological measurement of 3D calcaneus models from computed tomography images. Biomed Res 2019;30:149-59.
16. Schmutz B, Lüthi M, Schmutz-Leong YK, Shulman R, Platt S. Morphological analysis of Gissane's angle utilising a statistical shape model of the calcaneus. Arch Orthop Trauma Surg 2021;141:937-45.
17. Arifin WN. Sample size calculator, Date of access 15-03-2022. Available online: https://wnarifin.github.io/ssc/ssicc.html
18. Walter SD, Eliasziw M, Donner A. Sample size and optimal designs for reliability studies. Stat Med 1998;17:101-10.
19. Altman DG, Bland JM. Measurement in Medicine: The Analysis of Method Comparison studies. Statistician 1983;32:307-17.
20. Shrout PE, Fleiss JL. Intraclass correlations: uses in assessing rater reliability. Psychol Bull 1979;86:420-8.
21. Center of excellence SIGMA in mathematics & statistics support. 2022. Data of access: 05-04-2022. Available online: https://www.statstutor.ac.uk/resources/uploaded/coventryreliability.pdf
22. Koo TK, Li MY. A Guideline of Selecting and Reporting Intraclass Correlation Coefficients for Reliability Research. J Chiropr Med 2016;15:155-63.

Cite this article as: Wakker AM, Van Lieshout EMM, De Boer AS, Cornelissen BMW, Verhofstad MHJ, Van Walsum T, Visser JJ, Van Vledder MG. A novel method to perform morphological measurements on three-dimensional (3D) models of the calcaneus based on computed tomography (CT)-imaging. Quant Imaging Med Surg 2024. doi: 10.21037/qims-24-142